Journal of Medicinal Chemistry

ARTICLE

pubs.acs.org/jmc

Discovery and Structure−Activity Relationship of 3-Aminopyrid-2-ones as Potent and Selective Interleukin-2 Inducible T-Cell Kinase (Itk) Inhibitors†

Jean-Damien Charrier,*,‡ Andrew Miller,‡ David P. Kay,‡ Guy Brenchley,‡ Heather C. Twin,‡ Philip N. Collier,‡ Sharn Ramaya,‡ Shazia B. Keily,‡ Steven J. Durrant,‡ Ronald M. A. Knegtel,‡ Adam J. Tanner,§ Kieron Brown,§ Adam P. Curnock,§ and Juan-Miguel Jimenez‡

‡Department of Chemistry and §Department of Biology, Vertex Pharmaceuticals (Europe) Ltd., 88 Milton Park, Abingdon, Oxfordshire OX14 4RY, U.K.

Supporting Information

ABSTRACT: Interleukin-2 inducible T-cell kinase (Itk) plays a role in T-cell functions, and its inhibition potentially represents an attractive intervention point to treat autoimmune and allergic diseases. Herein we describe the discovery of a series of potent and selective novel inhibitors of Itk. These inhibitors were identified by structure-based design, starting from a fragment generated de novo, the 3-aminopyrid-2-one motif. Functionalization of the 3-amino group enabled rapid enhancement of the inhibitory activity against Itk, while introduction of a substituted heteroaromatic ring in position 5 of the pyridone fragment was key to achieving optimal selectivity over related kinases. A careful analysis of the hydration patterns in the kinase active site was necessary to fully explain the observed selectivity profile. The best molecule prepared in this optimization campaign, **7v**, inhibits Itk with a K_i of 7 nM and has a good selectivity profile across kinases.

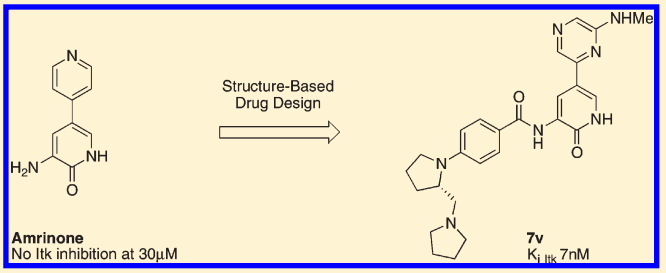

INTRODUCTION

The five Tec family tyrosine kinase members, Btk, Bmx, Itk, Rlk, and Tec, are expressed primarily in hematopoetic cells and have important roles in the development and function of leucocytes including B-cells, T-cells, and mast cells.[1] Three members of the Tec family, Itk, Rlk and Tec, are activated following antigen receptor engagement in T-cells and transmit signals to downstream effectors, including PLC-γ. A fourth member, Btk, appears to act independently of T-cell signaling and is essential for B-cell development and activation. A biological role for the final member of this family, Bmx, is not yet clearly elucidated.

Itk, a key member of this family, is predominantly expressed in T-cells, and a number of factors point to the importance of this kinase in immune diseases. Deletion of Itk in mice results in reduced T-cell receptor (TCR) induced proliferation and secretion of the cytokines IL-2, IL-4, IL-5, IL-10, and IFN-γ.[2−5] In Itk−/− mice, the immunological symptoms of allergic asthma are attenuated and lung inflammation, eosinophil infiltration, and mucous production are drastically reduced in response to challenge with the allergen ovalbumin.[6] Itk has also been implicated in atopic dermatitis. This gene has been reported to be more highly expressed in peripheral blood T-cells from patients with moderate and/or severe atopic dermatitis than in controls or patients with mild atopic dermatitis.[7]

This wealth of information on the role of Itk in T-cell function provides strong rationale for considering inhibition of this target to treat autoimmune and allergic diseases[8] and has prompted many pharmaceutical companies to initiate medicinal chemistry programs in order to identify small molecules Itk inhibitors.[9] BMS and BI have recently disclosed a series of 2-aminothiazoles[10,11] (e.g., **1** (BMS-509744)) and benzimidazoles[12−16] (e.g., **2**) as potent and selective Itk inhibitors (Figure 1). Compounds from these two scaffold families have been shown to be effective at inhibiting IL-2[17] and IL-4 production and lung inflammation in mice.[18]

An HTS campaign of our corporate compound collection led to the identification of potent Itk inhibitors from distinct scaffold series. However, these series showed cross-reactivity with a large proportion of our kinase counterscreening panel, and initial attempts to modify their selectivity profiles proved futile. Rather than deconvoluting these scaffolds back to the features required for their binding to Itk and then rebuilding potency/selectivity, we hypothesized that the likelihood of success would be enhanced by starting from a druglike, easy to derivatize hinge binding fragment.

In this report, we outline our efforts to identify a novel series of potent and selective Itk inhibitors from de novo design. The 3-aminopyrid-2-one fragment was selected as a core scaffold because of its potential ability to form a multiple hydrogen bond network with the hinge region of the ATP binding site of Itk similar to maleimides such as staurosporine and the CDK2 natural inhibitor hymenialdisine.[19−21] Compound **7v** represents the best molecule

Received: November 22, 2010
Published: March 10, 2011

dx.doi.org/10.1021/jm101499u | J. Med. Chem. 2011, 54, 2341–2350

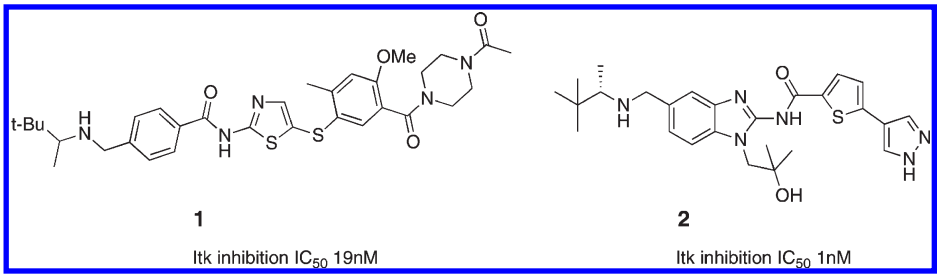

Figure 1. Structures of Itk inhibitors reported by Bristol Myers Squibb and Boehringer Ingelheim.

prepared in the pyridone series and shows inhibitory activity against Itk ($K_{i\,app}$ of 7 nM for Itk) comparable with compounds reported in the literature (e.g., **1** or **2**) and has a good selectivity profile.

CHEMISTRY

In order to rapidly optimize potency, selectivity, and physicochemical properties in the 3-aminopyrid-2-ones series, a synthetic route was required that would allow changes to the amide portion (R group) and C-5 (hetero)aryl (R′ group) in a flexible and efficient manner (Figure 2).

The general synthetic route that was developed is illustrated with the preparation of compound **7o** in Scheme 1.[22] The key boronate intermediate **4** is prepared from **3** using pinacoldiboronate in the presence of Pd as a catalyst.[23] Suzuki coupling with the appropriate heteroaryl halide partner affords **5**, which under Cbz deprotection and final acylation provides the final compound **7o**. The preparation of compound **7o** was performed in a highly efficient four-step sequence with an overall yield of 28% starting from easily accessible building blocks.

Compounds **7a**−**y** were all prepared using this highly versatile sequence.

Compound **11**, in which the amide functional group is connected to the pyridone through the carbonyl, is prepared as described in Scheme 2. Malondialdehyde **8** reacts with cyanoacetamide to generate intermediate **9**, which is further hydrolyzed into compound **10**. Amide coupling with the suitably functionalized aniline provides the final compound **11**.[19]

RESULTS AND DISCUSSION

To assess the potential of our de novo fragment approach, the commercially available vasodilator amrinone **12** was envisioned to be an excellent druglike starting point, as it combines a hinge binding 3-aminopyrid-2-one motif and offers a readily exploitable functionalization point to rapidly introduce diversity (amino group at position 3 of pyridone nucleus). A simple benzoyl capping of the exocyclic amine of fragment amrinone yielded the benzamide analogue **7a**, with micromolar potency against Itk and good ligand efficiency (20.2; LE = pK_i/MW) (Figure 3). As a hit compound, **7a** is likely to require 100- to 1000-fold potency improvement against Itk to become comparable to reported inhibitors in the literature (e.g., **1** and **2**).

An X-ray structure of compound **7a** (PDB code 3QGW) bound into the ATP binding site of Itk was determined with a resolution of 2.1 Å (Figure 4). This structure confirms the involvement of the aminopyridone binding motif in a network of hydrogen bonds with the hinge: the distance between the Glu436 backbone C═O and the endocyclic N−H is measured to be 2.7 Å, and the distance between the Met438 backbone N−H and the pyridone C═O is 2.3 Å. The longer distance of 4.0 Å between the Met438 backbone C═O and inhibitor exocyclic N−H suggests that only a weak third hydrogen

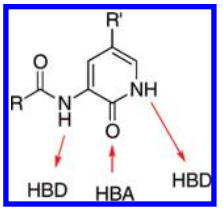

Figure 2. Generic structure for 3-aminopyrid-2-one series.

bond is formed with the hinge. Unexpectedly, the aromatic CH in the ortho-position of the benzamide moiety also seems to provide additional hydrogen bonding in the hinge region, as the X-ray reveals a distance of 3.9 Å with the Met438 backbone C═O. In addition to these contacts with the hinge, the pyridine ring disrupts a salt bridge formed between Lys391 and Asp500 that is observed in the Itk apo structure[24] and the aromatic nitrogen of the inhibitor rests within H-bond distance (3.5 Å) of the salt-bridge lysine 391. The pyridine ring itself is able to make an edge-to-face $\pi-\sigma$ interaction with Phe435 located at the back of the active site.

Analysis of this initial crystal structure also suggests that further hydrophobic interactions with residues Phe437 and Leu379, located above the hinge at the entrance of the active site, could be made from appropriate substitution on the benzamide ring. This ring, by virtue of its proximity to bulk solvent, would also be a suitable attachment point to allow introduction of solubilizing groups (Figure 4b).

Additional affinity and selectivity over other kinases might also be achieved by variation of the pyridine ring: alternative heteroaryls with appropriate subsitution are likely to alter interaction with the "gatekeeper" residue Phe435, which, though not unique to Itk, is not strongly conserved across kinases.

With the objective of transforming hit compound **7a** (K_i = 1.3 μM) into an inhibitor that would be more suitable for lead optimization, we initially examined variations of the amide, targeting the additional lipophilic contacts in this area of the active site (Table 1). Progress was monitored using inhibitory activity against Itk (K_i) and ligand efficiency (LE = pK_i/MW).

Reduction of the aromatic benzamide (compound **7b**) or introduction of a spacer group between the aromatic ring and the carbonyl amide (compound **7c**) resulted in a >20-fold loss of potency. These results are in line with the observation that the aromatic CH in the ortho-position of the benzamide **7a** forms a hydrogen-bond-like interaction with a hinge carbonyl and can be further rationalized by the proximity of the phenyl ring to Phe437 which may allow productive $\pi-\pi$ interaction.

Small lipophilic substitution on the benzamide ring was tolerated, preferably at position 4 (**7f**, K_i = 1.2 μM, LE = 19.4). The effect of larger hydrocarbon motifs in the para-position was therefore examined in a systematic fashion, and a small array of compounds showed that the inhibitory activity could improve

dx.doi.org/10.1021/jm101499u |J. Med. Chem. 2011, 54, 2341–2350

Scheme 1[a]

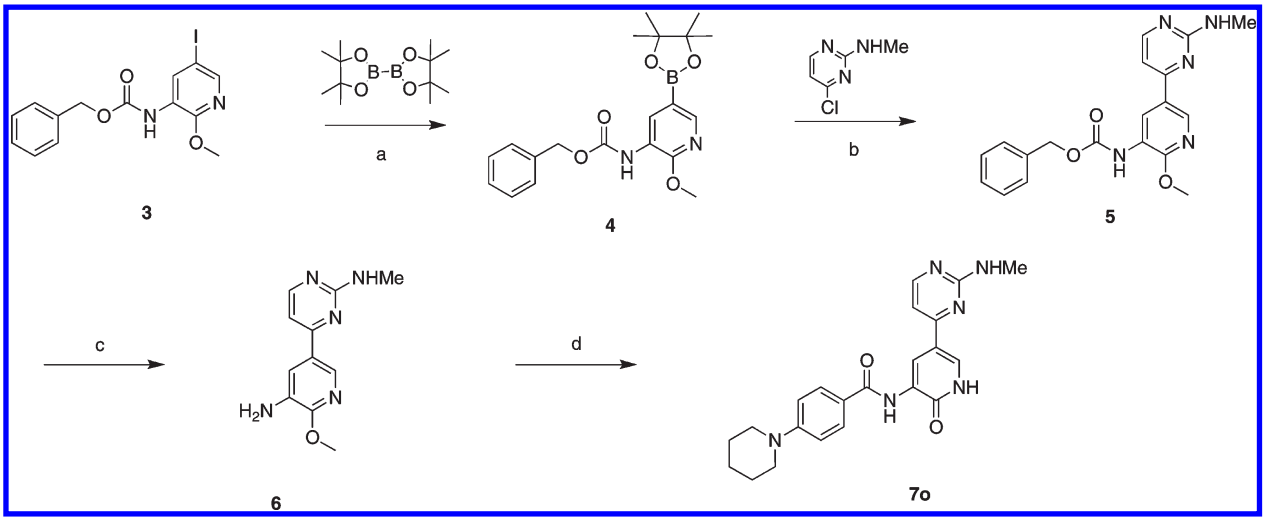

[a] Reagents and conditions: (a) $PdCl_2(PPh_3)_2$, KOAc, dioxane, 77%; (b) $Pd(PPh_3)_4$, Na_2CO_3, toluene/EtOH/water, 67%; (c) H_2, Pd/C, MeOH/AcOEt, 100%; (d) 4-(piperidin-1-yl)benzoic acid, $POCl_3$, MeCN, 55%.

Scheme 2[a]

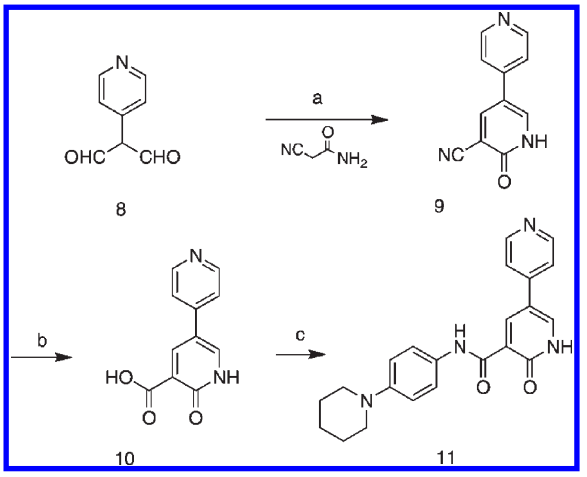

[a] Reagents and conditions: (a) morpholine, AcOH, benzene, 83%; (b) 9 N HCl, reflux, 54% ; (c) 4-(piperidin-1-yl)aniline, EDCI, Et_3N, DMF, 20%.

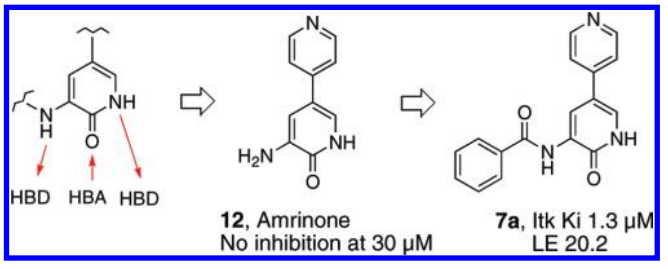

Figure 3. From de novo design to hit compound **7a**.

with increasing size of the lipophile while maintaining ligand efficiency. This culminated with a cyclohexyl group for which potency started to plateau and ligand efficiency to decrease (**7j**, K_i = 0.22 μM, LE = 17.8). This saturated six-membered ring was further modified and could be advantageously replaced with a piperidine ring (**7m**, K_i = 0.093 μM, LE = 18.8).

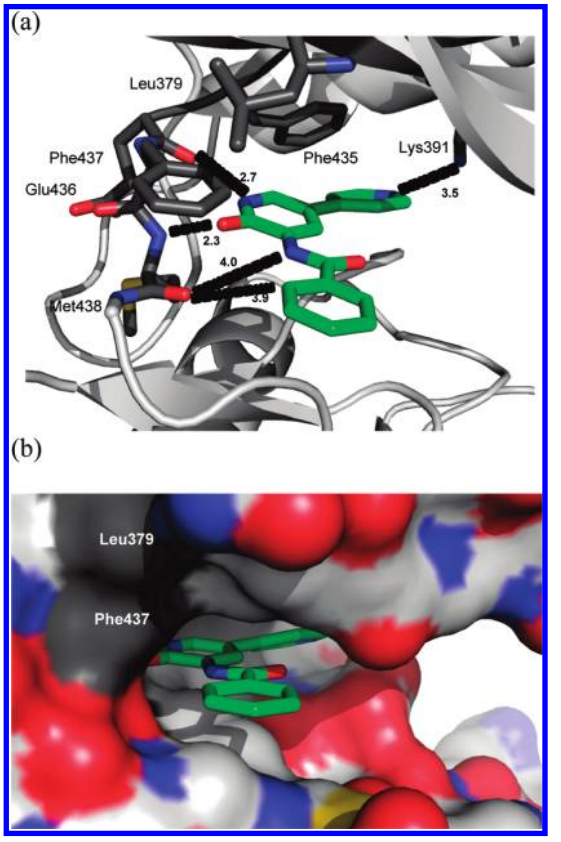

Figure 4. X-ray structure of compound **7a** in the Itk active site (RCSB Protein Data Bank code 3QGW). Itk crystal structures were visualized with Pymol, version 1.1r1 (Schrödinger LLC, NY, 2010). (a) X-ray structure of compound **7a** (green) in Itk active site (gray). Important residues, including those hydrogen-bonding to the ligand, are highlighted in stick. (b) Shape and chemical complementarity between the Itk active site (surface representation) and compound **7a** (green).

Reversing the amide linker between the pyridone core and the phenyl ring showed similar inhibitory activity (**11**, K_i = 0.14 μM vs **7m**, K_i = 0.093 μM), in agreement with our earlier observation

dx.doi.org/10.1021/jm101499u |J. Med. Chem. 2011, 54, 2341–2350

Table 1. Structures and Inhibitory Activity of Variants 7a−m and 11[a]

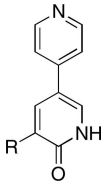

Compd	R	Itk Ki (μM)	LE
7a	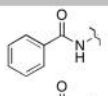	1.3	20.2
7b	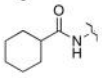	> 30	-
7c	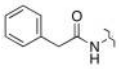	> 30	-
7d	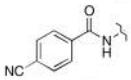	> 6*	-
7e	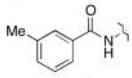	2.1	18.6
7f	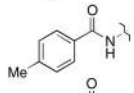	1.2	19.4
7g	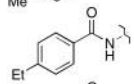	0.53	19.7
7h	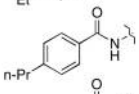	0.28	19.6
7i	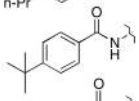	0.12	19.9
7j	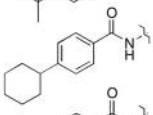	0.22	17.8
7k	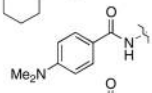	0.21	20.0
7l	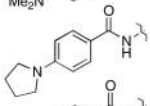	0.17	18.8
7m	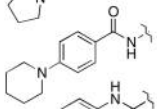	0.093	18.8
11	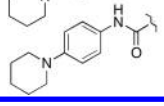	0.14	18.3

[a] Functionalization is at position 3. The asterisk (∗) indicates that the upper concentration of compound was limited by solubility in assay (15% inhibition at 3 μM).

that this NH does not make a strong hydrogen bond with Met438.

It was found empirically through our counterscreen panel of ∼20 diverses enzymes that compounds **7a**−**m** also inhibited a number of unrelated kinases (e.g., c-Kit, Flt3, and Src), and it became apparent that modification of the substitution pattern on the benzamide moiety did not significantly improve their selectivity profile (e.g., **7i** and **7k**: $K_{i\,Kit}$ = 27 and 46 nM, respectively; $K_{i\,Flt3}$ = 11 and 8 nM, respectively; $K_{i\,Src}$ = 1.32 and 2.8 μM, respectively). Starting from compound **7m**, we therefore initiated a second phase of the lead optimization campaign based on the hypothesis that selectivity might be modulated if interactions with residues that are deeply buried in the active site were altered (e.g., "gatekeeper" residue Phe435 and Asp500/Lys391 salt bridge residues).

Both residues Phe435 and Asp500 can potentially be accessed from substitution on the pyridine nucleus in **7m**; hence, we examined the effect of a methylamino substitution in position 2 of the pyridine nucleus (Table 2). Compound **7n** showed a 13-fold enhancement in potency (K_i = 7 nM) and improved ligand efficiency (LE = 20.2). Replacement of the 2-methylaminopyridine moiety with a 2-methylaminopyrimidine (compounds **7o**) led to a similar profile, in terms of both potency and selectivity.

An X-ray structure of **7o** (PDB code 3QGY) was determined with a resolution of 2.1 Å in order to understand the increase in affinity observed (Figure 5). Although originally expected to improve potency by introducing a new hydrogen bond to the salt-bridge Asp500, instead the methylamino group was found to promote conformational changes in nearby residues, resulting in the creation of a new lipophilic pocket. Changes include a small 10° rotation of the phenyl ring of Phe435, a major 160° rotation of the ε-methyl group of Met410, and the formation of a new hydrogen bond with Glu406 of the C-helix (Figure 5a). The methyl group ends up deeply buried in the newly formed pocket lined by the phenyl ring of Phe435 above and the side chains of Met410 and Val419 in the back and below, respectively (Figure 5b). The conformations of residues within van der Waals range of the aminomethylheteroaryl moiety were found to be conserved in subsequent crystal structures, independent of the nature of the heteroaryl ring (results not shown). Because of the vicinity of the methylamino substituent to the Glu406 carboxylate in the crystal structure (Figure 5), the hydrogen bond donating ability of the amino linker was considered to be key to the observed improvement in potency. Indeed, its replacement with a more lipophilic methanethiol group lost approximately 10-fold in affinity (results not shown). Given this SAR and the local environment observed in the crystal structure of **7o**, no further hydrophobic substitutions were attempted at this position. Attempts to further optimize interactions in this pocket using larger aminoalkyl groups resulted in a significant reduction in activity (**7r** vs **7s**, K_i = 0.112 μM and K_i > 2 μM, respectively), in agreement with the space available in the crystal structure and the rigidity of the Phe435 gatekeeper side chain that restricts the size of the pocket. No such induced-fit effects are required in the case of Src kinase where the methylamino group can fit into the existing Src-selectivity pocket; the addition of a methylamino group therefore also leads to a potency improvement in the case of Src. The local environment near the methylamino group in Kit and Flt3 is more challenging to interpret because, in contrast to Itk, several distinct inactive structures have been published and it is not clear to which conformation our inhibitors bind.[25−28]

In addition to the gain in potency via the methylamino group, the X-ray structure also reveals that the pyrimidine nitrogen is still 3.5 Å from Lys391, hence able to form a productive H-bond. This observation is in line with the significant potency reduction observed with compounds lacking the ring nitrogen acceptor in this position (**7n** vs **7q**, K_i = 7 and 145 nM, respectively).

In our investigation of the impact of variation of the heteroaryl at C5, the best results were obtained with compounds **7t** and **7u**, which retained good activity against Itk (K_i = 11 and 23 nM, respectively), in combination with an improved selectivity window with related

Table 2. Structures and Inhibitory Activity of Amide Variants 7m−u[a]

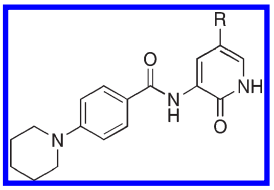

Compds	R	Itk Ki (μM)	LE	c-Kit Ki (μM)	Flt3 Ki (μM)	Src Ki (μM)
7m		0.093	18.8	0.012	0.032	1.80
7n		0.007	20.2	0.012	0.006	0.14
7o		0.016	19.3	< 0.010	0.005	0.04
7p		0.046	18.1	0.083	0.020	1.20
7q		0.145	17.0	0.081	0.080	0.22
7r		0.112	17.2	0.148	0.069	0.48
7s	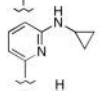	> 2.0	<13.2	-	0.120	> 4.0
7t		0.011	19.7	0.155	0.110	0.59
7u		0.023	18.9	0.27	1.045	0.59

[a] Functionalization is at position 5.

kinases (**7t** c-Kit K_i = 155 nM; Flt3 K_i = 110 nM; Src K_i = 590 nM; **7u** c-Kit K_i = 270 nM; Flt3 K_i = 1045 nM; Src K_i = 590 nM).

It is difficult to explain the data obtained for compounds **7t** and **7u**, since the aromatic nitrogens do not appear to make direct contact with residues in the active site. Commonly used computational methods failed to explain these results on the basis of crystallographic data, since moving a single aromatic nitrogen was predicted to lose the H-bond with Lys391 (or the equivalent catalytic lysine in other kinases), and as a result, a reduction in affinity was anticipated. This expectation was realized for Flt3, Kit, and Src (**7t** vs **7o**) where potency was reduced by 5- to 20-fold. However, in Itk this prediction did not hold true and binding affinities of **7t** and **7o** were very similar.

Given that direct protein−ligand contacts could not be used to provide a satisfactory explanation of the observed selectivity pattern, the possible role of solvation/desolvation was investigated.[29] Using the molecular dynamics tool Watermap, hydration sites in apo-Itk have been identified.[30] One particular hydration site, present in Itk and absent in Src, Flt3, and Kit, is found close to the position of the aromatic nitrogen in **7t** and **7u**. This hydration site in apo-Itk is predicted to be highly thermodynamically unfavorable; displacement of this water molecule with a suitable inhibitor could therefore provide an energy gain, resulting in improved potency against Itk but not against other kinases that lack this hydration site. The average orientation of water molecules at this hydration site suggests that an sp^2-nitrogen restores complementarity with the local solvent structure, in contrast to the corresponding CH analogue. This hypothesis is also consistent with the SAR of inhibitors **7t** and **7r**; **7t** possesses an sp^2-nitrogen which is complementary with solvent ($K_{i\,7t}$ = 11 nM) while **7r** does not, leading to a 10-fold loss in potency ($K_{i\,7r}$ = 112 nM).

In the case of compounds **7t** and **7u**, the loss of H-bond with Lys391 and the gain in potency through improved complementarity with the solvent structure in the Itk active site cancel each other, resulting in similar binding affinity to **7n** and **7o**.

To further explore this unique feature in the context of compounds with druglike solubility and cell permeability, a range of inhibitors with the solubilizing motif pyrrolidinomethylpyrrolidine were prepared (**7v**−**y**). The pyrrolidinomethylpyrrolidine moiety was identified by virtual screening of a library of commercially available amines against the Itk crystal structure, using Glide with SP scoring (Schrödinger LLC, NY, 2010). Inhibitors **7v**−**y** possess diverse H-bond acceptor features able to displace the Itk-specific water molecule (Table 3).

dx.doi.org/10.1021/jm101499u | J. Med. Chem. 2011, 54, 2341–2350

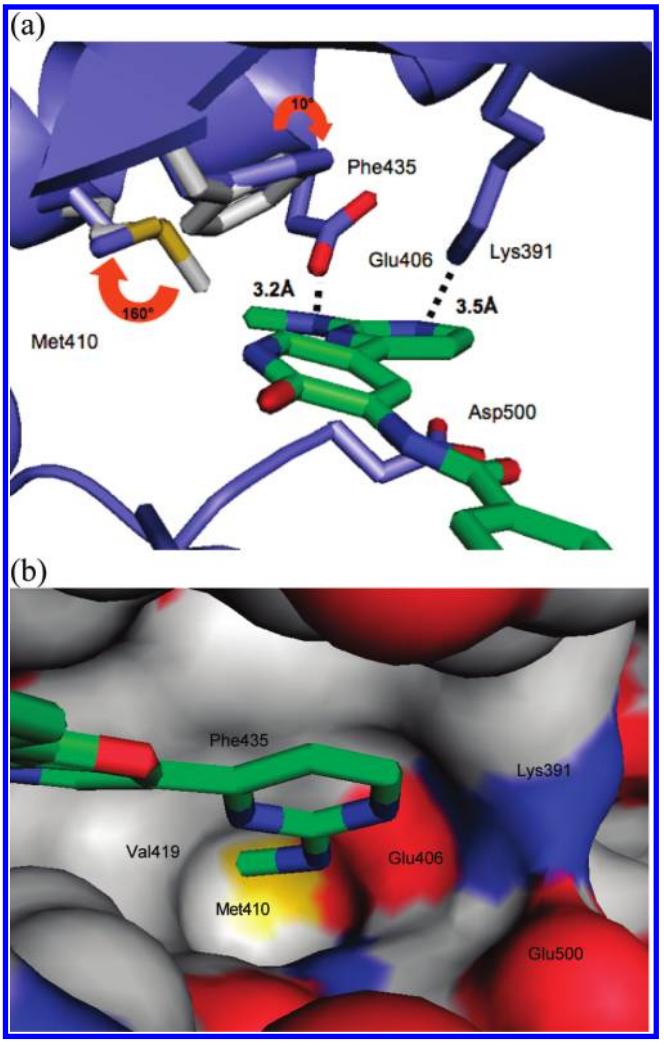

Figure 5. X-ray structure of compound **7o** in Itk active site (RCSB Protein Data Bank code 3QGY). (a) X-ray structure of compound **7o** (green) in Itk active site (purple). Important residues, including those involved in conformational changes, are highlighted as sticks. These conformational changes from the apo-enzyme (white) to the complex with **7o** (purple) are highlighted with orange arrows. Movements of Phe435 (small arrow) and Met410 (large arrow) enable the formation of a new lipophilic pocket. (b) X-ray structure of compound **7o** (green) in ATP binding site (surface representation). The methylamino group of **7o** fills a newly created pocket lined by Met410, Phe435, and Val419.

As expected, pyrimidine **7v** and pyridine **7w** had similar profiles to compounds **7t** and **7u** described above.

Replacement of the aromatic nitrogen H-bond acceptor in pyridine **7w** with an aromatic C−F H-bond acceptor[31] resulted in fluorophenyl derivative **7x** with retained inhibitory activity against Itk and good selectivity versus c-Kit, Flt3 and Src. As anticipated, the profile obtained for **7x** was completely different from that of compound **7q**, which cannot rely on the aromatic C−F (C−H instead) to fill the hydration site unique to Itk.

The nitrile hydrogen bond acceptor in cyanophenyl derivative **7y** is projected deeper into the active site and no longer overlays with the Itk-specific hydration site. To explain the retention of the selectivity profile, we hypothesize that the second solvation shell around the unique Itk hydration site may play a role. As the Itk-specific hydration site projects the oxygen atoms of occupying water molecules toward bulk solvent, nearby water molecules will orient their dipoles accordingly and project their own oxygen atoms toward subsequent solvation shells. The cyano nitrogen of **7y** could mimic the oxygen atoms of water molecules in the second solvation shell of the original hydration site, thus conserving the optimal solvent structure in the Itk active site.

In addition to retaining good potency and selectivity, compounds **7v**−**y** have been designed for their druglike properties (Table 3); all have solubility, lipophilicity, and permeability profiles that are consistent with good cell penetration. Of particular interest, compound **7v** shows good Itk affinity, selectivity, and physicochemical properties consistent with oral druglike characteristics (solubility at pH 7.4 is 150 μg/mL; good permeability with no major efflux as measured in Caco2 study, A−B 10.8 × 10^{-6} cm/s, B−A 32.4.10^{-6} cm/s) (Tables 3 and 4).

The best molecule prepared in this rapid optimization campaign, compound **7v**, has inhibitory activity against Itk comparable with compounds reported in the literature (e.g., BMS-509744)[9] and has a good selectivity profile across a representative panel of kinases. The kinases used to establish the extended selectivity profile of **7v** listed in Table 4 provide representative examples of kinases from all major groups of enzymatically active kinases as defined by Manning et al.[32] (assay data obtained using the Kinase Profiler service provided by Millipore, Billerica, MA, U.S.). Additionally, physicochemical properties of compound **7v** are consistent with good cell penetration. Compound **7v** therefore represents a good chemical probe for further mechanistic and structural investigations into the Itk pathway, results of which will be presented elsewhere.

CONCLUSION

A novel class of Itk inhibitors based on the 3-aminopyrid-2-one fragment was identified. Structure based design helped build in potency and rationalize the subtleties of the Itk SAR. Careful analysis of the hydration patterns in the kinase active sites helped to explain the selectivity that was observed and may prove to be a useful tool to engineer selectivity in future projects.

The discovery of compound **7v** illustrates the fact that a fragment-like de novo starting point can rapidly evolve into compounds with good potency and selectivity profile.

MATERIALS AND METHODS

General Experimental Details. All commercially available solvents and reagents were used as received. Microwave reactions were carried out using a CEM Discovery microwave. Analytical thin layer chromatography was carried out using glass-backed plates coated with Merck Kieselgel 60 GF_{240}. Plates were visualized using UV light (254 or 366 nm) and/or by staining with potassium permanganate followed by heating. Flash chromatography was carried out on an ISCO Combiflash Companion system, eluting with a 0−100% EtOAc/petroleum ether gradient. Samples were applied preabsorbed on silica. ^{1}H NMR and ^{13}C NMR spectra were recorded at 400 MHz using a Bruker DPX 400 instrument. HRMS spectra were recorded on a Waters Micromass Q Tof Premier spectrometer, operating in positive electrospray mode. MS samples were analyzed on a MicroMass Quattro Micro mass spectrometer operated in single MS mode with electrospray ionization. Samples were introduced into the mass spectrometer using chromatography. Infrared spectra were recorded in the range 4000−600 cm^{-1} using a Nicolet Avatar 360 FTIR spectrometer and were recorded neat. Elemental analysis was carried out on a Control Equipment Corporation 440 elemental analyzer. Melting points were measured on a Büchi B-545 electrothermal digital melting point apparatus and are uncorrected. All final products had a purity of ≥95%. The purity of final products was determined by either combustion analysis or HPLC. Combustion analyses were performed on a Control Equipment Corporation 440

Table 3. Structures, Selectivity Profiles, and Physicochemical Properties of Analogues 7v−y

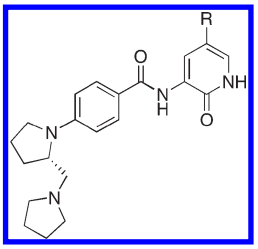

Compds	R	Itk Ki (μM)	c-Kit Ki (μM)	Flt3 Ki (μM)	Src Ki (μM)	solubility at pH7.4 (μg/mL)	logD	CaCo2 A-B / B-A (10^{-6} cm/s)
7v		0.007	0.2	0.02	0.12	150	2.8	10.8 / 32.4
7w		0.020	1.3	0.14	0.28	115	2.9	nd
7x		0.020	0.4	0.08	0.30	34	3.9	3.3 / 19.9
7y		0.027	0.4	0.41	0.48	23	3.9	3.3 / 16.4

Table 4. Extended Selectivity Profile of Compound 7v

primary target *Ki* (μM)		Other enzymes *Ki* (μM)									
Itk	0.007	Abl	> 1	Cot	> 1	Hck	> 1	Mkk6	> 1	Prk2	> 1
		Akt1	> 1	Csk	> 1	Ido1	> 1	Msk1	> 1	Ret	> 1
Enzymes in TCR pathway *Ki* (μM)		Ampk	> 1	Dyrk1A	> 1	Igf1R	> 1	Mst2	> 1	Rock2	> 1
		AurA	> 1	Egfr	> 1	Ikkα	> 1	Nek1	> 1	Ron	> 1
		Bmx	> 1	Ephb2	> 1	IR	> 1	P38α	> 1	Ros	> 1
Lck	0.49	Btk	> 1	Erbb4	> 1	Irak4	> 1	P38β	> 1	Rsk1	> 1
Erk1	> 2	Camk1D	> 1	Fak	> 1	Jak2	0.37	P70S6k1	> 1	Sgk1	> 1
Erk2	> 2	Camk4	> 1	Fer	> 1	Jak3	0.35	Pdgfrα	> 1	Src	0.12
Fyn	> 1	Cdk1	> 1	Fes	> 1	Jnk1	> 1	PDK	> 1	Tak1	0.86
Rlk	> 2	Chek1	> 1	Fgfr4	> 1	Kdr	0.43	Pim1	> 1	Tbk1	> 1
c-Raf	> 2	CerK	> 1	Flt3	0.02	Kit	0.2	Pkc-β	> 1	Tie2	> 1
Zap70	> 2	Chk1	> 1	Fms	> 1	LynA	> 1	Plk3	> 1	Yes	> 1
Pkc-θ	> 2	Ck1	> 1	Gsk3β	> 1	Mek1	> 1	Prak	> 1	Zipk	> 1

elemental analyzer. HPLC purity was measured on an Agilent HP1100 HPLC instrument with a Waters Quattro MS system equipped with an ACE C_8 reverse phase column (4.6 mm × 150 mm, 5 μm). The mobile phases were acetonitrile/methanol (1:1) and water (20 mM, pH 7.0, Tris phosphate).

3-Benzyloxycarbonylamino-5-(4,4,5,5-tetramethyl-1,3,2-dioxaborolan-2-yl)-(1*H*)-pyridin-2-one (4)[22]**.** A mixture of 3-benzyloxycarbonylamino-5-iodo-(1*H*)-pyridin-2-one **3** (100 g, 260.5 mmol, 1.0 equiv), bis(pinacolato)diboron (69.4 g, 273.3 mmol, 1.05 equiv), and potassium acetate (76.64 g, 780.8 mmol, 3.0 equiv) in anhydrous dioxane (900 mL) was degassed and flushed with nitrogen. $PdCl_2(PPh_3)_2$ (5.48 g, 7.8 mmol, 3 mol %) was added and the mixture heated to reflux overnight. After the mixture was cooled to ambient temperature, the solvent was removed in vacuo, the residue was dissolved in ethyl acetate, washed with aqueous brine, and dried ($MgSO_4$), and the solvent was removed in vacuo. The crude product was purified by column chromatography, eluting with 20% ethyl acetate/petroleum ether to give, after concentration, an orange solid. This was treated with *n*-heptane (500 mL) and heated to reflux. On cooling the resultant precipitate was collected by filtration and washed with hexane to give **4** as a golden solid (77.3 g, 201 mmol, 77%): mp 105.1−106.2 °C; ^{1}H NMR ($CDCl_3$) δ 1.35 (12H, s), 4.02 (3H, s), 5.24 (2H, s), 7.20 (1H, s), 7.43−7.40 (5H, m), 8.21 (1H, s), 8.65 (1H, s); ^{13}C NMR ($CDCl_3$) δ 25.2, 27.3, 54.2, 67.6, 84.3, 122.5, 128.7, 128.8, 129.0, 130.7, 136.4, 147.1, 153.6, 155.3; IR 2935, 1719, 1533, 1476, 1438, 1359, 1254, 1216, 1141, 1049, 757, 687; ES M + H 385.20, M − H 383.18. Anal. Calcd for $C_{20}H_{25}BN_2O_5$: C, 62.52; H, 6.56; N, 7.29. Found: C, 62.60; H, 6.59; N, 6.96.

dx.doi.org/10.1021/jm101499u |*J. Med. Chem.* 2011, 54, 2341–2350

Table 5. Parameters for Itk, c-Kit, and Flt-3 Kinase Activity Assays

assay	[kinase] (nM)[d]	target peptide	[peptide][d]	[ATP] (mM)[d]	μCi [γ-^{33}P]ATP per nmol of ATP	time course (min)
Itk[a]	25	SAM68[e]	3 μM	0.08	200	40
c-Kit[b]	30	poly Glu/Tyr (4:1)	0.5 mg/mL	1.4	4	45
Flt-3[c]	1	poly Glu/Tyr (4:1)	0.5 mg/mL	0.09	25	20

[a] Assay buffer: 20 mM MOPS (pH 7), 10 mM $MgCl_2$, 1 mM DTT, 0.1% BSA. [b] Assay buffer: 100 mM HEPES (pH 7.5), 10 mM $MgCl_2$, 25 mM NaCl, 1 mM DTT, 0.01% BSA. [c] Assay buffer: 100 mM HEPES (pH 7.5), 10 mM $MgCl_2$, 25 mM NaCl, 1 mM DTT, 0.01% BSA. [d] Final assay concentration. [e] Src-associated in mitosis 68 kDa protein, residues 332−443.

General Procedure for the Formation of Suzuki Adducts: 3-Benzyloxycarbonylamino-5-(2-(methylamino)pyrimidin-4-yl)-(1*H*)-pyridin-2-one (5). 3-Benzyloxycarbonylamino-5-(4,4,5,5-tetramethyl-1,3,2-dioxaborolan-2-yl)-(1*H*)-pyridin-2-one **4** (357 mg, 0.929 mmol, 1.0 equiv) was dissolved in toluene (15 mL) and ethanol (3 mL). 4-Chloro-*N*-methylpyrimidin-2-amine (160 mg, 1.11 mmol, 1.2 equiv) was added, followed by $Pd(PPh_3)_4$ (54 mg, 0.046 mmol, 5 mol %), sodium carbonate (679 mg, 6.41 mmol, 6.9 equiv), and water (6 mL). The mixture was heated to reflux for 2 h. After cooling, the reaction mixture was diluted with water and extracted three times with ethyl acetate. The combined organics were washed with brine, dried ($MgSO_4$), and filtered, and the solvent was removed under reduced pressure. The crude product was purified by flash chromatography on silica, eluting with 40−70% ethyl acetate/petroleum ether to give **5** as a yellow solid (227 mg, 0.62 mmol, 67%): ^{1}H NMR (DMSO-d_6) δ 2.82 (3H, s), 3.94 (3H, s), 5.17 (2H, s), 7.06 (1H, d), 7.11−7.19 (1H, m), 7.29−7.35 (5H, m), 8.30 (1H, s), 8.58 (1H, s), 8.69 (1H, s), 9.10 (1H, s). MS *m*/*z*: 366.8 $(M + H)^+$.

General Procedure for Cbz Deprotection: 3-Amino-5-(2-(methylamino)pyrimidin-4-yl)-(1*H*)-pyridin-2-one (6). A solution of 3-benzyloxycarbonylamino-5-(2-(methylamino)pyrimidin-4-yl)-(1*H*)-pyridin-2-one **5** (200 mg, 0.548 mmol, 1.0 equiv) in ethyl acetate (30 mL) and methanol (30 mL) was degassed under nitrogen, and 10% Pd/C (40 mg, 20 wt %) was added. The mixture was stirred under an atmosphere of hydrogen for 16 h before being filtered through a pad of Celite, which was washed with methanol. The filtrate was concentrated under reduced pressure to give **6** as a viscous oil (125 mg, quantitative yield): ^{1}H NMR (DMSO-d_6) δ 2.86 (3H, d), 3.92 (3H, s), 5.15 (2H, br s), 6.98 (1H, d), 7.03 (1H, d), 7.56 (1H, br s), 8.09 (1H, s), 8.26 (1H, s). MS *m*/*z*: 232.7 $(M + H)^+$.

General Procedure for the Preparation of Final Compounds 7a−y: 3-(4-(Piperidin-1-yl)benzoylamino)-5-(2-(methylamino) pyrimidin-4-yl)-(1*H*)-pyridin-2-one (7o). To a solution of 4-(piperidin-1-yl)benzoic acid (129 mg, 0.628 mmol, 1.0 equiv) in acetonitrile (15 mL) was added 3-amino-5-(2-(methylamino)pyrimidin-4-yl)-(1*H*)-pyridin-2-one **6** (145 mg, 0.628 mmol, 1.0 equiv) followed by phosphoryl chloride (117 μL, 1.256 mmol, 2.0 equiv), and the mixture was heated to reflux for 6 h. After the mixture was cooled, the solvent was removed under reduced pressure and 2 M NaOH was added to the residue, followed by the addition of 2 M HCl. The precipitate that formed was collected by filtration, washed with water, and then recrystallized from methanol to give 3-(4-(piperidin-1-yl)benzoylamino)-5-(2-(methylamino)pyrimidin-4-yl)-(1*H*)-pyridin-2-one **7o** (163 mg, 0.40 mmol, 55%).

(*S*)-3-(4-(2-(Pyrrolidin-1-ylmethyl)pyrrolidin-1-yl)benzoylamino)-5-(6-(methylamino)pyrazin-2-yl)-(1*H*)-pyridin-2-one (7v). ^{1}H NMR (DMSO-d_6) δ 1.69 (br s, 4H), 1.90−2.08 (m, 4H), 2.37−40 (m, 1H), 2.40−2.45 (m, 1H), 2.59 (br d, 2H), 2.87 (d, 3H), 2.96 (br s, 2H), 3.12−3.19 (m, 1H), 3.41−3.45 (m, 1H), 3.93 (br s, 1H), 6.66 (d, 2H), 7.08−7.11 (m, 1H), 7.75−7.79 (m, 3H), 7.84−7.86 (m, 1H), 8.08 (s, 1H), 8.98 (d, 1H), 9.04 (s, 1H), 12.42 (d, 1H). MS *m*/*z*: 474.4 $(M + H)^+$. HRMS calcd for $C_{26}H_{32}N_7O_2$, 474.2619; found, 474.2612.

(1*H*)-Pyridin-2-ones 7a−y. Analytical data are provided in the Supporting Information.

3-Cyano-5-(pyridin-4-yl)-(1*H*)-pyridin-2-one (9). To a stirred solution of 2-(pyridin-4-yl)malondialdehyde **8** (Acros Organics, 20 g, 134.2 mmol, 1.0 equiv) in benzene (500 mL) was added at ambient temperature 2-cyanoacetamide (12.41 g, 147.5 mmol, 1.1 equiv), morpholine (14.73 mL, 169 mmol, 1.26 equiv), and acetic acid (16 mL, 281.3 mmol, 2.1 equiv). The reaction mixture was heated to reflux for 24 h with azeotropic removal of water using a Dean−Stark water separator. The reaction mixture was cooled to ambient temperature and stirred for an additional 24 h. The precipitated solid was isolated by filtration, washed with ethyl acetate, and dried in vacuo. The crude product was triturated from acetonitrile and the resultant precipitate isolated by filtration to give **9** as a brown solid (22.0 g, 111.7 mmol, 83%). ^{1}H NMR (DMSO-d_6) δ 7.60 (2H, d), 8.26 (1H, s), 8.52 (2H, d), 8.59 (1H, s), 12.2 (1H, br s). MS *m*/*z*: 198.2 $(M + H)^+$.

3-Carboxy-5-(pyridin-4-yl)-(1*H*)-pyridin-2-one (10). A solution of 3-cyano-5-(pyridin-4-yl)-(1*H*)-pyridin-2-one **9** (22.0 g, 111.7 mmol, 1.0 equiv) in 9 N aqueous HCl (750 mL) was heated at reflux for 18 h. The reaction mixture was concentrated in vacuo and the residue triturated from acetone. The resultant precipitate was isolated by filtration, washed with acetone followed by ethanol, and dried in vacuo to give **10** as a yellow solid (13 g, 60.1 mmol, 54%). ^{1}H NMR (DMSO-d_6) δ 8.21 (2H, d), 8.64 (1H, s), 8.77 (2H, d), 8.82 (1H, d), 14.0 (1H, br s). MS *m*/*z*: 217.2 $(M + H)^+$.

3-(4-(Piperidin-1-yl)phenylcarbamoyl)-5-(pyridin-4-yl)-(1H)-pyridin-2-one (11). To a solution of 3-carboxy-5-(pyridin-4-yl)-(1*H*)-pyridin-2-one **10** (303 mg, 1.4 mmol, 1.0 equiv) in dry DMF (5 mL) were added at ambient temperature HOBT (236 mg, 1.54 mmol, 1.1 equiv) and TEA (234 μL, 1.68 mmol, 1.2 equiv) followed by EDCI (295 mg, 1.54 mmol, 1.1 equiv). After the mixture was stirred for 15 min, 4-(piperidin-1-yl)aniline (296 mg, 1.68 mmol, 1.2 equiv) was added and the reaction mixture was heated at 50 °C for 15 h. The reaction mixture was diluted with water and the precipitated solid isolated by filtration and washed successively with water, acetone, and diethyl ether. After drying *in vacuo*, compound **11** was isolated as a yellow solid (105 mg, 0.28 mmol, 20%). ^{1}H NMR (DMSO-d_6) δ 1.48−1.68 (6H, m), 3.05−3.15 (4H, m), 6.93 (2H, d), 7.56 (2H, d), 7.72 (2H, d), 8.36 (1H, d), 8.61 (2H, d), 8.80 (1H, d), 11.90 (1H, s), 13.20 (1H, brs). MS *m*/*z*: 375.5 $(M + H)^+$. HRMS calcd for $C_{22}H_{23}N_4O_2$, 375.1823; found, 375.1834.

Kinase Inhibition Assays. *Materials and Reagents.* HEPES, MOPS, NaCl, $MgCl_2$, BSA, ATP, TCA, NADH, poly Glu/Tyr, and DMSO were supplied by Sigma-Aldrich. DTT was from Melford Laboratories. Phosphenol pyruvate, pyruvate kinase, and lactate dehydrogenase were purchased from Roche diagnostics. Stock 3 mCi/mmol [γ-^{33}P]ATP and Optiphase Supermix scintillation cocktail were supplied by PerkinElmer. Unifilter GF/C filter plates were from PerkinElmer.

Itk, c-Kit, and Flt-3 Kinase Inhibition Assays. Ability of compounds to inhibit Itk, c-Kit, or Flt-3 kinase activity was tested using a radiometric phosphate incorporation assay as described in Table 5 and below.

A stock solution was prepared consisting of the appropriate buffer, kinase, and target peptide. To this was added the compound of interest at varying concentrations in DMSO to a final DMSO concentration of 3%. Assays were initiated by addition of an appropriate [γ-^{33}P]ATP solution and incubated at 25 °C. Assays were stopped, after the desired time course, by addition of TCA

and ATP to a final concentration of 10% and 0.2 mM, respectively. Peptides were captured on a Unifilter GF/C filter 96-well plate prepared according to the manufacturer's instructions and washed three times with 200 μL of 5% TCA prior to addition of 50 μL of scintillation cocktail and scintillation counting on a 1450 Microbeta liquid scintillation counter (Perkin Elmer). Dose-response data were analyzed using GraphPad Prism software (version 3.0cx for Macintosh, GraphPad software).

Src Kinase Inhibition Assay. Reactions were carried out at 30 °C in a total volume of 67 μL in a reaction buffer containing 25 mM HEPES (pH 7.5), 20 mM $MgCl_2$, 2 mM DTT, 280 μM NADH, 1 mM phosphoenol pyruvate, 30 μg/mL pyruvate kinase, 10 μg/mL lactate dehydrogenase, 3% DMSO, 50 μM ATP, 0.3 mg/mL poly Glu/Tyr (4:1), 25 nM Src, and serially diluted inhibitor compounds. Initial rate data were determined from the rate of change of absorbance at 340 nM (corresponding to stoichiometric consumption of NADH) using a Molecular Devices Spectramax plate reader (Sunnyvale, CA) over 10 min at 30 °C. Dose-response data were analyzed using GraphPad Prism software (version 3.0cx for Macintosh, GraphPad software).

■ ASSOCIATED CONTENT

Supporting Information. Analytical data for **7a**−**y**, summary of biological evaluation for **7a**−**y** and **11**, and details of the assays used. This material is available free of charge via the Internet at http://pubs.acs.org.

Accession Codes

†Coordinates of **7a** and **7o** cocrystallized with Itk have been submitted to the RCSB Protein Data Bank (PDB codes 3QGW and 3QGY, respectively).

■ AUTHOR INFORMATION

Corresponding Author

*Phone: + 44 (0) 1235 438800. Fax: + 44 (0) 1235 820440. E-mail: jean-damien_charrier@vrtx.com.

■ ACKNOWLEDGMENT

We thank C. Hudson, C. Memmott, C. Stuver-Moody, P. Wang, and J. Westcott for support with biochemical studies, G. Cheetham for structural information, the entire Itk project team, and S. Young for valuable discussions.

■ ABBREVIATIONS USED

ATP, adenosine 5′-triphosphate; Bmx, bone marrow tyrosine kinase gene in chromosome X protein; Btk, Bruton's tyrosine kinase; BI, Boehringer Ingelheim; BMS, Bristol-Myers Squibb; Cbz, carbobenzyloxy; CDK2, cyclin-dependent kinase 2; Flt3, FMS-like tyrosine kinase 3; HTS, high throughput screening; IFN-γ, interferon-γ; IL-2, interleukin-2; IL-4, interleukin-4; IL-5, interleukin-5; IL-10, interleukin-10; Itk, interleukin-2 inducible T-cell kinase; LE, ligand efficiency; PLC-γ, phospholipase C γ; Rlk, resting lympho cyte kinase; Tec, tyrosine kinase expressed in hepatocellular carcinoma; TCR, T-cell receptor; SAR, structure−activity relationship

■ REFERENCES

(1) Berg, L. J.; Finkelstein, L. D.; Lucas, J. A.; Schwartzberg, P. L. Tec family kinases in T lymphocyte development and function. *Annu. Rev. Immunol.* **2005**, *23*, 549–600.

(2) Liao, X. C.; Littman, D. R. Altered T cell receptor signaling and disrupted T cell development in mice lacking Itk. *Immunity* **1995**, *3*, 757–769.

(3) Fowell, D. J.; Shinkai, K.; Liao, X. C.; Beebe, A. M.; Coffman, R. L.; Littman, D. R.; Locksley, R. M. Impaired NFATc translocation and failure of Th2 development in Itk-deficient CD4+ T cells. *Immunity* **1999**, *11*, 399–409.

(4) Schaeffer, E. M.; Debnath, J.; Yap, G.; McVicar, D.; Liao, X. C.; Littman, D. R.; Sher, A.; Varmus, H. E.; Lenardo, M. J.; Schwartzberg, P. L. Requirement for Tec kinases Rlk and Itk in T cell receptor signaling and immunity. *Science* **1999**, *284*, 638–641.

(5) Schaeffer, E. M.; Yap, G. S.; Lewis, C. M.; Czar, M. J.; McVicar, D. W.; Cheever, A. W.; Sher, A.; Schwartzberg, P. L. Mutation of Tec family kinases alters T helper cell differentiation. *Nat. Immunol.* **2001**, *2*, 1183–1188.

(6) Mueller, C.; August, A. Attenuation of immunological symptoms of allergic asthma in mice lacking the tyrosine kinase ITK. *J. Immunol.* **2003**, *170*, 5056–5063.

(7) Matsumoto, Y.; Oshida, T.; Obayashi, I.; Imai, Y.; Matsui, K.; Yoshida, N. L.; Nagata, N.; Ogawa, K.; Obayashi, M.; Kashiwabara, T.; Gunji, S.; Nagasu, T.; Sugita, Y.; Tanaka, T.; Tsujimoto, G.; Katsunuma, T.; Akasawa, A.; Saito, H. Identification of highly expressed genes in peripheral blood T cells from patients with atopic dermatitis. *Int. Arch. Allergy Immunol.* **2002**, *129*, 327–340.

(8) Sahu, N.; August, A. ITK inhibitors in inflammation and immune-mediated disorders. *Curr. Top. Med. Chem.* **2009**, *9*, 690–703.

(9) Lo, H.-Y. Itk inhibitors: a patent review. *Expert Opin. Ther. Pat.* **2010**, *20*, 459–469.

(10) Das, J.; Chunjian, L.; Moquin, R. V.; Lin, J.; Furch, J. A.; Spergel, S. H.; McIntyre, K. W.; Shuster, D. J.; O'Day, K. D.; Penhallow, B.; Hung, C.-Y.; Kanner, S. B.; Lin, T.-A.; Dodd, J. H.; Barrish, J. C.; Wityak, J. Discovery and SAR of 2-amino-5-[(thiomethyl)aryl]thiazoles as potent and selective Itk inhibitors. *Bioorg. Med. Chem. Lett.* **2006**, *16*, 2411–2415.

(11) Das, J.; Furch, J. A.; Liu, C.; Moquin, R. V.; Lin, J.; Spergel, S. H.; McIntyre, K. W.; Shuster, D. J.; O'Day, K. D.; Penhallow, B.; Hung, C.-Y.; Doweyko, A. M.; Kamath, A.; Zhang, H.; Marathe, P.; Kanner, S. B.; Lin, T.-A.; Dodd, J. H.; Barrish, J. C.; Wityak, J. Discovery and SAR of 2-amino-5-(thioaryl)thiazoles as potent and selective Itk inhibitors. *Biorg. Med. Chem. Lett.* **2006**, *16*, 3706–3712.

(12) Snow, R. J.; Abeywardane, A.; Campbell, S.; Lord, J.; Kashem, M. A.; Khine, H. H.; King, J.; Kowalski, J. A.; Pullen, S. S.; Roma, T.; Roth, G. P.; Sarko, C. R.; Wilson, N. S.; Winters, M. P.; Wolak, J. P.; Cywin, C. L. Hit-to-lead studies on benzimidazole inhibitors of ITK: discovery of a novel class of kinase inhibitors. *Biorg. Med. Chem. Lett.* **2007**, *17*, 3660–3665.

(13) Moriarty, K. J.; Winters, M.; Qiao, L.; Ryan, D.; DesJarlis, R.; Robinson, D.; Cook, B. N.; Kashem, M. A.; Kaplita, P. V.; Liu, L. H.; Farrell, T. M.; Khine, H. H.; King, J.; Pullen, S. S.; Roth, G. P.; Magolda, R.; Takahashi, H. Itk kinase inhibitors: initial efforts to improve the metabolical stability and the cell activity of the benzimidazole lead. *Bioorg. Med. Chem. Lett.* **2008**, *18*, 5537–5540.

(14) Moriarty, K. J.; Takahashi, H.; Pullen, S. S.; Khine, H. H.; Sallati, R. H.; Raymond, E. L.; Woska, J. R., Jr.; Jeanfavre, D. D.; Roth, G. P.; Winters, M. P.; Qiao, L.; Ryan, D.; DesJarlais, R.; Robinson, D.; Wilson, M.; Bobko, M.; Cook, B. N.; Yin, Lo, H.; Nemoto, P. A.; Kashem, M. A.; Wolak, J. P.; White, A.; Magolda, R. L.; Tomczuk, B. Discovery, SAR and X-ray structure of 1*H*-benzimidazole-5-carboxylic acid cyclohexyl-methyl-amides as inhibitors of inducible T-cell kinase (Itk). *Bioorg. Med. Chem. Lett.* **2008**, *18*, 5545–5549.

(15) Cook, B. N.; Bentzien, J.; White, A.; Nemoto, P. A.; Wang, J.; Man, C. C.; Soleymanzadeh, F.; Khine, H. H.; Kashem, M. A.; Kugler, S. Z., Jr.; Wolak, J. P.; Roth, G. P.; De Lombaert, S.; Pullen, S. S.; Takahashi, H. Discovery of potent inhibitors of interleukin-2 inducible T-cell kinase (ITK) through structure-based drug design. *Bioorg. Med. Chem. Lett.* **2009**, *19*, 773–777.

(16) Winters, M. P.; Robinson, D. J.; Khine, H. H.; Pullen, S. S.; Woska, J. R., Jr.; Raymond, E. L.; Sellati, R.; Cywin, C. L.; Snow, R. J.; Kashem, M. A.; Wolak, J. P.; King, J.; Kaplita, P. V.; Liu, L. H.; Farrell, T. M.; DesJarlais, R.; Roth, G. P.; Takahashi, H.; Moriarty, K. J. 5-Aminomethyl-1*H*-benzimidazoles as orally active inhibitors of

inducible T-cell kinase (Itk). *Bioorg. Med. Chem. Lett.* **2008**, *18*, 5541–5544.

(17) Riether, D.; Zindell, R.; Kowalski, J. A.; Cook, B. N.; Bentzien, J.; De Lombaert, S.; Thomson, D.; Kugler, S. Z., Jr.; Skow, D.; Martin, L. S.; Raymond, E. L.; Khine, H. H.; O'Shea, K.; Woska, J. R., Jr.; Jeanfavre, D.; Sellati, R.; Ralph, K. L. M.; Ahlberg, J.; Labissiere, G.; Kashem, M. A.; Pullen, S. S.; Takahashi, H. 5-Aminomethylbenzimidazoles as potent ITK antagonists. *Bioorg. Med. Chem. Lett.* **2009**, *19*, 1588–1591.

(18) Lin, T. A.; McIntyre, K. W.; Das, J.; Liu, C.; O'Day, K. D.; Penhallow, B.; Hung, C. Y.; Whitney, G. S.; Shuster, D. J.; Yang, X.; Townsend, R.; Postelnek, J.; Spergel, S. H.; Lin, J.; Moquin, R. V.; Furch, J. A.; Kamath, A. V.; Zhang, H.; Marathe, P. H.; Perez-Villar, J. J.; Doweyko, A.; Killar, L.; Dodd, J. H.; Barrish, J. C.; Wityak, J.; Kanner, S. B. Selective Itk inhibitors block T-cell activation and murine lung inflammation. *Biochemistry* **2004**, *43*, 11056–11062.

(19) Li, R.; Xue, L.; Zhu, T.; Jiang, Q.; Cui, X.; Yan, Z.; McGee, D.; Wang, J.; Gantla, V. R.; Pickens, J. C.; McGrath, D.; Chucholowski, A.; Morris, S. W.; Webb, T. R. Design and synthesis of 5-aryl-pyridone-carboxamides as inhibitors of anaplastic lymphoma kinase. *J. Med. Chem.* **2006**, *49*, 1006–1015.

(20) Kuethe, J.; Wong, A.; Davis, I. W. Rapid and efficient synthesis of 1*H*-indol-2-yl-1*H*-quinolin-2-ones. *Org. Lett.* **2003**, *5*, 3975–3978.

(21) Kiethe, J. Y.; Wong, A.; Qu, C.; Smitrovitch, J.; Davies, I. W.; Hughes, D. L. Synthesis of 5-substituted-1*H*-indol-2-yl-1*H*-quinolin-2-ones: a novel class of KDR kinase inhibitors. *J. Org. Chem.* **2005**, *70*, 2555–2567.

(22) Durrant, S. J.; Pinder, J. L.; Charrier, J.- D.; Jimenez, J.- M.; Brenchey, G.; Collier, P. N.; Kay, D.; Miller, A.; Pierard, F.; Ramaya, S.; Sadiq, S.; Twin, H. Synthesis of a stable pyridyl boronate and its reaction with aryl and heteroaryl halides. *Heterocycles* **2006**, *70*, 509–517.

(23) Zhu, L.; Duquette, J.; Zhang, M. An improved preparation of arylboronates: application in one-pot Suzuki biaryl synthesis. *J. Org. Chem.* **2003**, *68*, 3729–3732.

(24) Brown, K.; Long, J. M.; Vial, S. C.; Dedi, N.; Dunster, N. J.; Renwick, S. B.; Tanner, A. J.; Frantz, J. D.; Fleming, M. A.; Cheetham, G. M. Crystal structures of interleukin-2 tyrosine kinase and their implications for the design of selective inhibitors. *J. Biol. Chem.* **2004**, *279*, 18727–32.

(25) Gajiwala, K. S.; Wu, J. C.; Christensen, J.; Deshmukh, G. D.; Diehl, W.; DiNitto, J. P.; English, J. M.; Greig, M. J.; He, Y. A.; Jacques, S. L.; Lunney, E. A.; McTigue, M.; Molina, D.; Quenzer, T.; Wells, P. A.; Yu, X.; Zhang, Y.; Zou, A.; Emmett, M. R.; Marshall, A. G.; Zhang, H. M.; Demetri, G. D. KIT kinase mutants show unique mechanisms of drug resistance to imatinib and sunitinib in gastrointestinal stromal tumor patients. *Proc. Natl. Acad. Sci. U.S.A.* **2009**, *106*, 1542–1547.

(26) Mol, C. D.; Dougan, D. R.; Schneider, T. R.; Skene, R. J.; Kraus, M. L.; Scheibe, D. N.; Snell, G. P.; Zou, H.; Sang, B. C.; Wilson, K. P. Structural basis for the autoinhibition and STI-571 inhibition of c-Kit tyrosine kinase. *J. Biol. Chem.* **2004**, *279*, 31655–31663.

(27) Mol, C. D.; Lim, K. B.; Sridhar, V.; Zou, H.; Chien, E. Y.; Sang, B. C.; Nowakowski, J.; Kassel, D. B.; Cronin, C. N.; McRee, D. E. Structure of a c-kit product complex reveals the basis for kinase transactivation. *J. Biol. Chem.* **2003**, *278*, 31461–31464.

(28) Griffith, J.; Black, J.; Faerman, C.; Swenson, L.; Wynn, M.; Lu, F.; Lippke, J.; Saxena, K. The structural basis for autoinhibition of FLT3 by the juxtamembrane domain. *Mol. Cell* **2004**, *13*, 169–178.

(29) Abel, R.; Young, T.; Farid, R.; Berne, B. J.; Friesner, R. A. Role of the active-site solvent in the thermodynamics of factor Xa ligand binding. *J. Am. Chem. Soc.* **2008**, *130*, 2817–2831.

(30) Knegtel, R. M. A.; Robinson, D. Unpublished results.

(31) Howard, J. A. K.; Hoy, V. J.; O'Hagan, D.; Smith, G. T. How good is fluorine as a hydrogen bond acceptor?. *Tetrahedron* **1996**, *52*, 12613–12622.

(32) Manning, G.; Whyte, D. B.; Martinez, R; Hunter, T.; Sudarsanam, S. The protein kinase complement of the human genome. *Science* **2002**, *298*, 1912–1934.